



# Non-linear and state-dependent effects of behavioral intervention on glioma progression and survival

Alexandra I. Bulava<sup>1,2,a</sup> , Vera V. Kudelkina<sup>1,3</sup> , Vladimir D. Ilyushichev<sup>1</sup> , Mikhail V. Gulyaev<sup>4</sup> ,  
Natalia A. Chistova<sup>1</sup> , Vladimir B. Dorokhov<sup>5</sup> , Zhanna A. Osipova<sup>6</sup> , and Yuri I. Alexandrov<sup>1</sup> 

<sup>1</sup> Shvyrkov Laboratory of Neuronal Bases of Mind, Institute of Psychology, Russian Academy of Sciences, Moscow, Russia129366

<sup>2</sup> Department of Life Sciences, Moscow Institute of Psychoanalysis, Moscow, Russia121170

<sup>3</sup> Laboratory of Neuromorphology, Avtsyn Research Institute of Human Morphology of FSBSI Petrovsky National Research Centre of Surgery, Moscow, Russia117418

<sup>4</sup> Department of Chemistry, Lomonosov Moscow State University, Moscow, Russia119991

<sup>5</sup> Laboratory of Sleep/Wake Neurobiology, Institute of Higher Nervous Activity and Neurophysiology, Russian Academy of Sciences, Moscow, Russia117865

<sup>6</sup> Department of Biology, University of Padua, Padua 35121, Italy

Received 30 December 2025 / Accepted 16 February 2026

© The Author(s), under exclusive licence to EDP Sciences, Springer-Verlag GmbH Germany, part of Springer Nature 2026

**Abstract** The impact of behavioral interventions on cancer progression is recognized as significant yet poorly understood, with high outcome variability suggesting a key role for individual predispositions. We hypothesize that therapeutic efficacy stems not only from the motor component of an intervention per se, but also from the essential role of positive motivational engagement during learning. Using an intracerebral C6 glioma model in Long–Evans rats, we found that the baseline anxiety level served as a powerful, non-linear predictor of disease outcome. The highest anxiety scores were associated with the most aggressive tumor growth and the lowest survival. We evaluated how a food-acquisition learning task, administered pre- or post-tumor implantation, modulated this relationship. The intervention attenuated the predictive power of baseline anxiety for tumor progression by improving outcomes in a subset of high-anxiety subjects while worsening them in some with normal anxiety, thereby converging their trajectories. Therefore, failing to account for this nonlinear relationship between baseline anxiety and treatment response can lead to erroneous conclusions in research and to clinical interventions that are, on average, ineffective. Our findings indicate that the outcome of a behavioral intervention—shaped by an individual’s psycho-neuro-immune traits and the intervention’s motivational context—can remodel the tumor microenvironment. The organism’s baseline psychophysiological phenotype sets the initial conditions. A positive motivational context can counteract stress-induced states, leading to a systemic neuroendocrine-immune recalibration that remodels the tumor microenvironment’s immune landscape. Thus, we argue for a paradigm shift toward personalized adjuvant strategies based on neuro-immunological profiling, motivated engagement, and controlled stress dynamics.

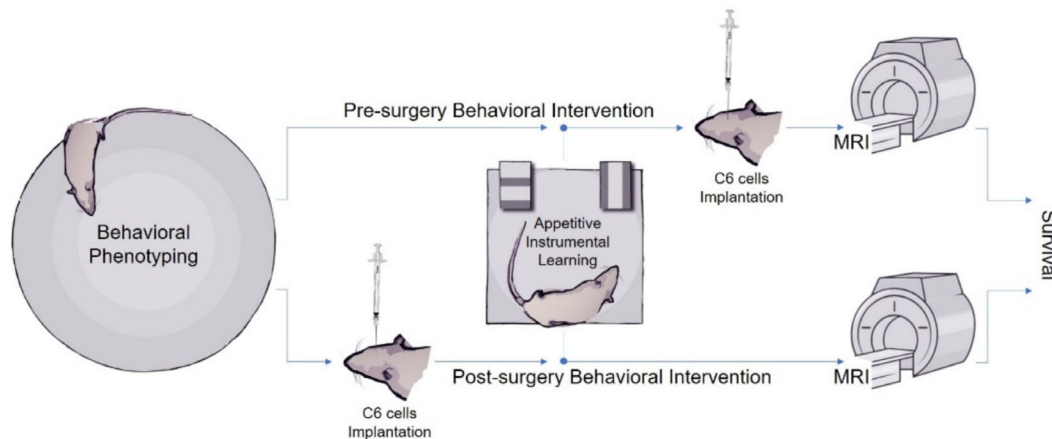
## 1 Introduction

### 1.1 Theoretical framework: systemogenesis, stress, and cellular adaptation

By expanding theoretical–evolutionary approaches to development, the theory of systemogenesis provides a powerful conceptual framework. It explains how the formation of functional systems—through coordinated gene expression, epigenetic regulation, and cellular phenotypic plasticity—determines the morphofunctional organization of tissues and their microenvironment [1–3]. From this perspective, cellular activity is anticipatory and oriented toward future outcomes. Cells cooperate to secure essential metabolites, and an inability to meet these demands triggers cellular plasticity—a morphofunctional restructuring [1, 4]. We propose that the nature of these adaptations varies

<sup>a</sup> e-mail: [bulavaai@ipran.ru](mailto:bulavaai@ipran.ru) (corresponding author)

## Graphical abstract



with the behavioral context, where stress intensity is a primary determinant [3, 5]. Applying this framework to an oncological context, tumor tissue can be conceptualized as a form of cellular adaptation. Its progression is driven by similar principles of coordinated molecular and cellular reorganization. The organism's basal psychophysiological phenotype, mediated via neuroendocrine and immune pathways, may act as a key system-forming factor that modulates this process and ultimately shapes the immune landscape of the tumor microenvironment [4]. Stress and anxiety share interrelated neurobiological bases [6] and are associated with cognitive deficits, particularly neocortical dysfunction [3, 5]. Our previous work demonstrated that experience-dependent mismatch during instrumental learning induces layer-specific changes in Fos (AP-1 transcription factor subunit) activity within the neocortex. Specifically, increased anxiety-like behavior correlated with a reduction in activated neurons in layers V–VI of the retrosplenial dysgranular cortex (RSD), whereas increased exploratory activity correlated with heightened activation in these same deep layers, but not in superficial layers I–III [7]. These findings support the view that phylogenetically older systems related to behavioral components such as locomotion are represented in the deep neocortical layers (V–VI), which form earlier in ontogeny. In contrast, the superficial layers (I–III), which develop later, are associated with more highly differentiated experiences involving additional environmental attributes. A characteristic feature of states induced by stress, high emotional intensity, or some pharmacological agents is this reversible *dedifferentiation*, often manifested as a reduction in behavioral complexity and a shift in cortical activity patterns [3, 5, 8, 9].

Although the strict biogenetic law that "ontogeny recapitulates phylogeny" is not entirely consistent with modern developmental biology, the fundamental relationship between phylogenetic and ontogenetic sequences remains evident. In the mammalian neocortex, early-born neurons populate the deepest layers, while later-born neurons migrate past them to form the superficial layers [10]. Notably, these later-born, superficial neurons are less resistant to damaging factors. For example, acute intoxication with nerve agents typically induces neuronal necrosis in superficial layers I–III of the neocortex and piriform cortex [11], which aligns with Ribot's law of retrograde amnesia (1881).

Mismatch between expectation and experience is a hallmark of conditions such as stress, intoxication, and learning. These states share a common mechanism of reversible dedifferentiation, manifested as a shift toward ontogenetically "older" memory systems, a blocking of "younger" memories, and a narrowing of attention. This adaptive process is interpreted as an evolutionarily conserved survival mechanism. Thus, stress promotes a shift from complex, differentiated behaviors to the implementation of simpler actions [8, 9, 12].

Our conclusions align with the hypothesis that interventions like "exercise" or "cognitive tasks" can induce activity-dependent gene programs across cell types, potentially driving a functional "rejuvenation" of cellular phenotypes through modifications of epigenetic regulators and the transcription of immediate-early genes (IEGs) [13]. Consequently, the dedifferentiation process described here is also reflected at the level of gene expression underlying adaptive behavioral modifications. Individual variations in these responses may stem from differences in pre-experimental experience, which shape how the brain implements such modifications. Using mathematical modeling, we have previously demonstrated that stress-induced dedifferentiation can accelerate learning in a novel task by deactivating existing experience that is unsuitable for the new context, thereby sharpening focus on the immediate demands [8, 9].

## 1.2 Psychoneuroimmunological mechanisms linking chronic stress to cancer

Stress-induced plasticity aligns with atavistic models of oncogenesis, which posit cancer as an inverse recapitulation of development [14]. Exposure to survival-relevant novelty can induce a transient cellular dedifferentiation-like phenotype, reverting cells to a more plastic, progenitor-like state [13, 15]. Cell stressors promote a transition to a stem-like state, enabling new adaptive states via chromatin remodeling [16]. A key mechanism involves chronic stress-driven glucocorticoid receptor (GR) activation, which programs cellular phenotypes and functional epigenomic patterns [17, 18], potentially contributing to oncogenic processes like the CpG island hyper-methylated phenotype [18, 19]. Critically, processes such as DNA recombination can lead to the cell's adaptive history "fixation" [20], meaning that restoration of a differentiated state occurs within the constraints of these changes. If the aggressiveness of the tumor is rooted in this ancient, resilient plasticity, then treatment strategies should shift from merely destroying dividing cells toward managing the state of differentiation and the niche microenvironment, in order to transition tumor cells from a resilient stem-like state to a more vulnerable, differentiated one.

A principal mechanism linking stress to oncogenesis is neuroendocrine dysregulation. The growing prominence of the biopsychosocial model and the emergence of cancer neuroscience have intensified the focus on the mechanisms linking psychological states to tumor development [21, 22]. Acute stress mobilizes energy by upregulating glucose metabolism and redistributes immune cells (natural killer cells, cytotoxic lymphocytes) from reservoirs to peripheral tissues. This augments immune surveillance and may potentiate antitumor immunity, creating a less permissive tumor microenvironment (TME) [23]. In contrast, sustained activation of the stress axis releases glucocorticoids and catecholamines (e.g., noradrenaline), which directly promote tumor proliferation and foster an immunosuppressive TME [24, 25].

Chronic stress, anxiety, and depression are common in cancer patients and can promote tumor growth and worsen outcomes [26, 27]. On a molecular level, these effects are largely mediated by noradrenaline and cortisol. Noradrenaline promotes tumorigenic processes via  $\beta$ -adrenergic receptor signaling [28, 29]. Sustained adrenergic signaling can induce tumor cell production of brain-derived neurotrophic factor (BDNF) in an ADRB3/cAMP/EPAC/JNK-dependent manner, promoting intra-tumoral nerve growth and creating a self-amplifying pro-tumor circuit [30]. Glucocorticoids, whose dysregulation is linked to anxiety and depression [31], exert potent immunosuppressive effects that can facilitate tumor progression [18, 32]. Glucocorticoid exposure upregulates factors like Tsc22d3, which blocks antigen presentation and interferon response [26]. Another immunosuppressive mechanism involves stress-induced tryptophan degradation via the indoleamine-2,3-dioxygenase (IDO) pathway, promoting regulatory T cell expansion [27].

In glioma, these mediators can disrupt genomic stability by inducing p53 degradation via  $\beta$ 2-adrenergic receptor ( $\beta$ 2-AR) and GR signaling [25, 33, 34]. Stress hormones also alter microglial homeostasis [35] and drive metabolic reprogramming, activating glycolytic enzymes and lipolysis to supply tumors with energy and biosynthetic precursors [36, 37]. This is complemented by gut microbiota dysbiosis, characterized by reduced microbial diversity and protective short-chain fatty acids (SCFAs), which triggers systemic inflammation [38–40]. Chronic neuroinflammation and DNA damage are hypothesized central mechanisms of cancer and cancer-related cognitive impairment, with potential biomarkers including damage-associated molecular patterns (DAMPs), circulating microRNAs, and exosomes. Collectively, these pathways underscore chronic stress as a significant modulator of cancer biology, with preclinical evidence confirming its role in promoting tumor progression [41].

However, a central challenge is the significant individual variation in stress severity and cancer susceptibility. This heterogeneity suggests that an individual's pre-existing behavioral experience may be a critical determinant. Neuroscience data challenge strict functional localization, showing that individual experience is represented across distributed cortical-subcortical networks [42, 43]. Tools like c-Fos mapping reveal that brain activity patterns, such as neocortex activity levels, differ based on an individual's experience and the degree of mismatch between expected and actual outcomes [15, 44], highlighting the neural basis of individual variability.

The benefits of physical exercise in cancer prevention and therapy, alongside the adverse effects of physical inactivity, are well-documented [45]. A key mechanistic focus has been on motor activity per se and its systemic consequences, including the engagement of the dopaminergic system and the secretion of myokines and muscle-specific miRNAs (myomiRs) from contracting skeletal muscle. These factors are known to modulate the tumor microenvironment (TME), creating conditions for cancer progression [45, 46].

However, we hypothesize that the primary therapeutic mechanism may not reside in the "motor component" itself. We consider this component merely one facet of holistic behavior, which can be simultaneously described from different perspectives: perceptual, motivational, emotional, and others. We propose that the critical factor is the recruitment of distributed cellular elements into a systemogenesis with positive valence and motivation, driven by the behavioral context of the intervention. This framework could explain the considerable variability in therapeutic outcomes reported across studies [46], which may stem from individual differences in stress sensitivity and from which specific motivation-driven experiential domain (approach or avoidance) is engaged by a given experimental paradigm [3].

### 1.3 Purpose and study objectives

Highly differentiated brain structures are more vulnerable to stress, whereas tumors, by co-opting archaic survival programs, become more adaptive and resilient under such conditions. Conventional aggressive therapy disproportionately affects these "young" neural systems and creates a selective pressure that favors the most resistant and malignant clones. Therefore, a therapeutic strategy targeting phenotypic plasticity—specifically, forcing the differentiation of tumor cells into a more mature, less aggressive state—combined with active neuroprotection may prove more effective.

While the molecular pathways linking stress to cancer are increasingly mapped, the predictive power of individual behavioral phenotypes—specifically, pre-existing anxiety-like behavior—on tumor progression dynamics remains poorly characterized. Furthermore, it is unclear how a behavioral intervention with positive valence might modulate this relationship, potentially offsetting the negative impact of a high-anxiety phenotype.

To test this hypothesis, we focused on individual behavioral phenotypes and their interaction with a valenced behavioral intervention in a glioma model. The primary objective of this study was to investigate the relationship between baseline anxiety-like behavior and glioma progression, and to determine how this relationship is modulated by an appetitive instrumental learning task.

An experimental design was implemented where C6 glioma cells [47, 48] were stereotactically implanted intracerebrally into Long–Evans rats. Animals first underwent behavioral phenotyping [7] to assess baseline anxiety and exploratory activity. They were then subjected to an appetitive food-acquisition learning task [7, 49, 50], administered either before or after tumor induction, to serve as a behavioral intervention with positive valence.

## 2 Materials and methods

### 2.1 Experimental subjects and housing

#### 2.1.1 Animals

50 adult Long–Evans hooded rats (20 females, 30 males), aged 5–9 months, was used in this study. The body weight ranged from 210 to 285 g for females and 300 to 480 g for males. The animals were housed in groups in standard laboratory cages (46 × 30 × 16 cm) under a 12/12-h light/dark cycle at an ambient temperature of  $23 \pm 1$  °C, with ad libitum access to water. To maintain a controlled motivational state, food restriction was implemented, ensuring that body weight did not fall below 80% of the free-feeding level.

#### 2.1.2 Compliance with ethical standards

All experimental procedures were conducted in strict accordance with the National Institutes of Health "Guidelines for the Care and Use of Animals for Experimental Procedures" and were approved by the Bioethics Commissions of the Avtsyn Research Institute of Human Morphology (Petrovsky National Research Centre of Surgery) and the Institute of Psychology of the Russian Academy of Sciences. It was conducted in compliance with Directive 2010/63/EU of the European Parliament and of the Council on the protection of animals used for scientific purposes. The minimum number of animals required for statistical significance was used, and all efforts were made to minimize suffering.

### 2.2 Behavioral tasks

Prior to tumor inoculation, animals underwent sequential behavioral phenotyping to assess baseline exploratory activity and anxiety-like behavior using modified open field and novel object recognition tests (Fig. 1a). The experimental timeline (Fig. 1b) incorporated appetitive instrumental learning (food-acquisition task) as a behavioral intervention, administered either before or after C6 glioma cells intracerebral implantation via stereotactic surgery.

#### 2.2.1 Modified open field test (mOFT)

Spontaneous motor and exploratory activity were assessed in an open field apparatus. The test was conducted in a round arena (diameter 50 cm) with uniform illumination of 40–45 lx. A key modification to the standard protocol was the application of additional lighting in the central area. Each rat was placed in the chamber and allowed to explore freely for 5 min. The following behaviors were recorded and analyzed: freezing, grooming, horizontal activity (distance traveled), and vertical activity (rearing).

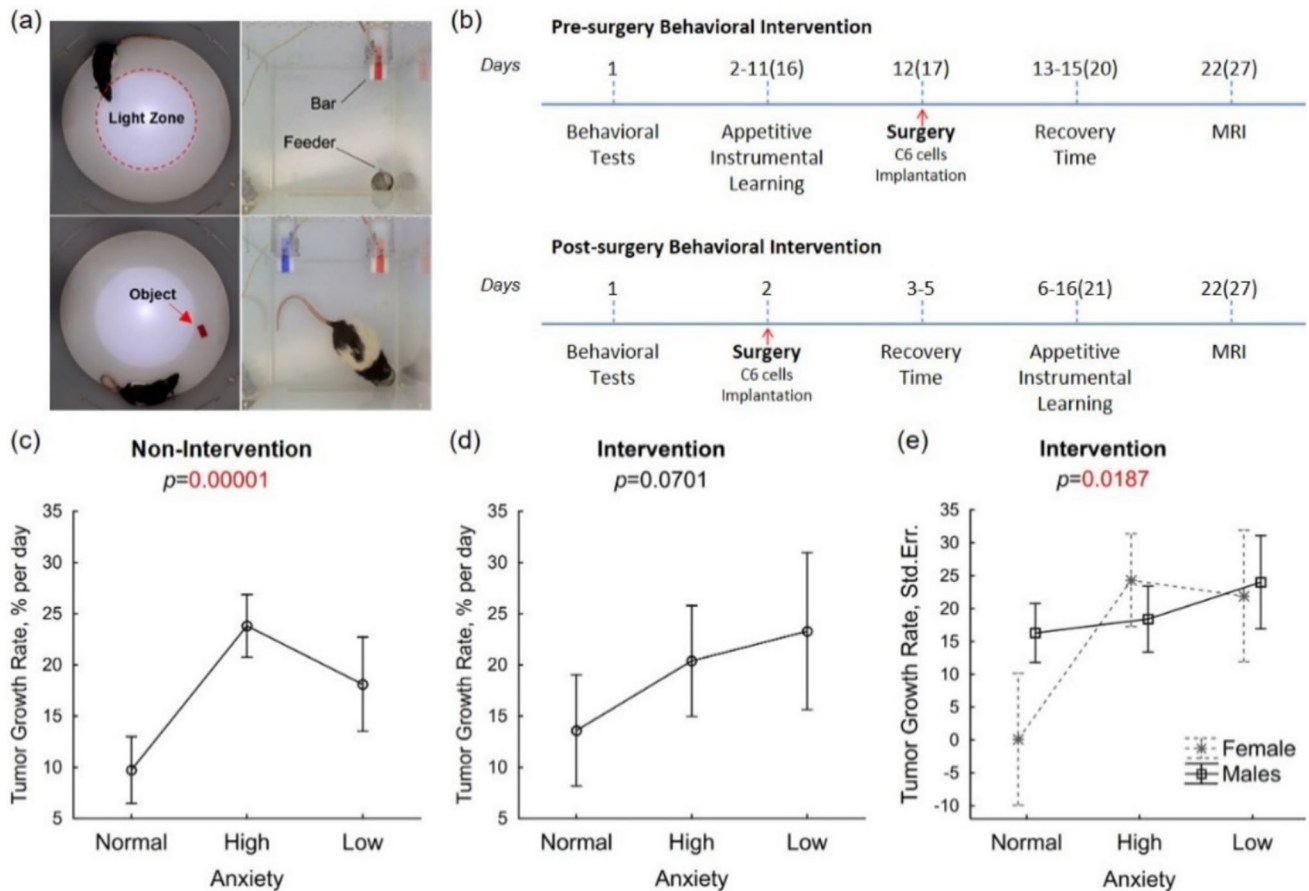


**Fig. 1** Behavioral phenotyping, experimental timeline, and the relationship between anxiety-like behavior and glioma progression rate. **a** Representative video frames from behavioral phenotyping (left panel: modified Open Field Test (mOFT, top) and Novel Object Recognition Test (mNORT, bottom)) and operant food acquisition (right panel). **b** Experimental timeline outlining pre- and post-surgical behavioral interventions. **c–e** Relationship between baseline anxiety-like behavior levels and glioma progression rate (**c**) in the non-intervention group, ANOVA:  $F(2, 18) = 21.94$ ,  $p < 0.001$ ; Bonferroni post hoc: High versus Normal,  $p < 0.001$ ; High versus Low,  $p = 0.132$ ; Normal versus Low,  $p = 0.017$ . Kruskal–Wallis:  $H(2, N = 21) = 16.129$ ,  $p < 0.001$ , High versus Normal,  $p = 0.0002$ . **d** in the intervention group, ANOVA:  $F(2, 12) = 3.34$ ,  $p = 0.07$ . Kruskal–Wallis:  $H(2, N = 13) = 5.318$ ,  $p = 0.07$ . **e** in the intervention cohort, analyzed by sex, ANOVA:  $F(2, 9) = 6.39$ ,  $p = 0.019$ ; Bonferroni post hoc: Normal females versus High females,  $p = 0.018$ ; Normal females versus Low males,  $p = 0.019$ ; Normal females versus Normal males,  $p = 0.117$ . For the latter comparison, Tukey's test yielded  $p = 0.066$ ; Normal females versus High males,  $p = 0.053$  per Bonferroni, while Tukey's test yielded  $p = 0.032$ . Kruskal–Wallis's test showed no significant differences

### 2.2.2 Modified novel object recognition test (mNORT)

The NORT is based on the natural tendency of animals to explore novelty. This test was performed in the same chamber as the OFT. A key modification was introduced during the test phase: the novel object was placed unexpectedly on the side of the arena opposite to the animal's current location. Recorded behavioral variables included the freeze response upon novel object presentation, latency to initiate movement (for all four paws), and object-directed behaviors (sniffing, manipulation with paws or mouth).

### 2.2.3 Appetitive instrumental learning

Animals were trained in a food-acquisition task in a  $25 \times 25 \times 50$  cm experimental chamber equipped with an automatic feeder, which was triggered by a lever press. Chamber illumination was maintained at 30–35 lx during sessions. Training consisted of daily 30-min sessions. The behavioral cycle for food acquisition comprised the following sequential acts: pressing the lever, lowering the head into the feeder, and retrieving the food pellet. Training continued until a stable performance level was achieved. The instrumental task was considered acquired once an animal performed ten consecutive cycles (designated as learning criterion). If an animal failed to meet the

criterion on a given day, training was repeated the following day. Following skill acquisition, animals practiced the task for a minimum of five additional days. Consequently, the total training duration ranged from 10 to 15 days.

To control for the potential confounding effect of nutritional regimen between the behavioral intervention groups (deprivation and food reward), animals in the no-intervention group were divided into two subgroups: (a) those subjected to dietary restriction matching the intervention groups deprivation schedule and fed an equivalent amount of the same pellets used as a reward ( $n = 9$ ); (b) those housed under standard vivarium conditions with ad libitum access to food and water ( $n = 20$ ).

### 2.2.4 Behavioral recording and analysis

All behavioral test sessions were video-recorded. The duration(s) of each behavioral event was scored offline using RealTimer software (RPC Open Science Ltd). Anxiety-like behavior was assessed based on specific behavioral patterns in accordance with established ethological models [51, 52]. Data from instrumental learning acquisition were analyzed using custom software developed by S.V. Volkov [50].

## 2.3 Tumor model and in vivo procedures

### 2.3.1 Cell culture

Rat C6 glioma cells were sub-cultured in DMEM medium supplemented with 2 mM glutamine (PanEco), 10% fetal bovine serum (FBS, Capricorn Scientific), 10 U/mL penicillin, and 10  $\mu$ g/mL streptomycin (PanEco). The cells were cultured in 75 cm<sup>2</sup> flasks (Fudau Biotechnology) at 37 °C in a humidified atmosphere with 5% CO<sub>2</sub> (Sanyo). For sub-culturing, cells were detached using 0.25% trypsin–EDTA (PanEco), and cell viability was assessed by trypan blue exclusion (0.4%) in a Goryaev chamber. Only cell preparations with a viability of  $\geq 96\%$  were used for subsequent experiments.

### 2.3.2 Neurosurgical procedure

Rat C6 glioma cells were implanted using an optimized stereotactic technique. The animals were anesthetized with an intraperitoneal injection of a cocktail comprising Zoletil (tiletamine and zolazepam, Virbac Sante Animale, France; 25 mg/kg) and Rometar (xylazine 2%, Spofa, Czech Republic; 10 mg/kg) and secured in a stereotaxic apparatus. A midline scalp incision was made, and a burr hole was drilled into the cranial bone. C6 glioma cells ( $1 \times 10^5$  in 5  $\mu$ L of RPMI-1640 medium without glutamine) were injected into the right frontal lobe using a Hamilton syringe at the following stereotaxic coordinates: 3 mm anterior and 1 mm lateral to the right of the bregma, at a depth of 2 mm from the dura mater. The injection was performed at a rate of 0.5  $\mu$ L/min. The needle was left in place for 5 min before being slowly withdrawn to minimize backflow. Finally, the skin incision was sutured. Postoperatively, the animals were placed on a heating pad maintained at 37 °C to facilitate recovery from anesthesia.

### 2.3.3 Magnetic resonance imaging (MRI)

MRI was performed in vivo on days 20–23 of C6 glioma growth using a 7 T MRI scanner (BioSpec 70/30 USR; Bruker BioSpin, Germany) for small laboratory animals, operated by the ParaVision® v.5.1 software and equipped with a gradient system achieving 105 mT/m. Anesthesia was induced and maintained with isoflurane (Laboratorios Karizoo, Spain) using a 4.5% concentration for induction in a chamber and 1.5% for maintenance via a nasal mask. Axial T1-weighted images were obtained immediately after intravenous administration of the contrast agent Gadovist® (Bayer AG, Germany) at a dose of 0.25 mmol/kg of gadobutrol per animal. For injection, 0.1 mL of the commercial 1.0 M formulation was diluted with 0.2 mL of 0.9% NaCl to achieve a final volume of 0.3 mL. 2D FLASH (Fast Low-Angle Shot) pulse sequence was used with the following scan parameters: field of view (FOV) =  $2.6 \times 2.6$  cm<sup>2</sup>, matrix =  $200 \times 200$ , in-plane resolution =  $0.13 \times 0.13$  mm<sup>2</sup>, slice thickness = 0.8 mm, number of slices = 16, number of averages = 4, repetition time (TR) = 268.8 ms, echo time (TE) = 7.3 ms, flip angle (FA) = 60°, bandwidth = 25 kHz, and acquisition time = 3 min 35 s.

### 2.3.4 Tumor size calculation

Cross-sectional tumor areas were delineated semi-automatically on individual MR slices and quantified using Image Pro Plus 3.0 software (Media Cybernetics Inc., USA). Total tumor volume (mm<sup>3</sup>) was subsequently calculated based on these data using Excel (Microsoft, USA). The analysis encompassed both the peri-tumoral contrast-enhancing rim and the central hypointense areas, indicative of necrotic tissue.

### 2.3.5 Specific tumor growth rate, SGR

The specific growth rate of glioma was calculated to quantitative characterization [53] using the logarithmic difference in size over a period, expressed as a percentage per day:

$$\text{SGR} = (\ln(\text{SE}) - \ln(\text{SB})) \times 100/t,$$

where SGR is the specific growth rate (%); SB is the tumor size at the beginning of the period; SE is the tumor size at the end of the period;  $t$  is the period length (days).

## 2.4 Statistical analysis

Statistical analysis and data visualization were performed using Statistica 12.0 (StatSoft Inc., USA) and Python 3.12.9. A  $p$  value  $< 0.05$  was considered statistically significant.

For comparisons of variables across groups, parametric one-way or factorial analysis of variance (ANOVA) was the primary method. Given the small sample size in several experimental groups, which limits the reliability of normality tests, the non-parametric Kruskal–Wallis  $H$  test was also applied as a robust alternative. Following a significant ANOVA result, post hoc pairwise comparisons were conducted using Tukey’s HSD test. The Bonferroni correction was applied for planned pairwise comparisons where appropriate. Comparisons against a single control group were performed using Dunnett’s test. For significant Kruskal–Wallis results, pairwise differences were assessed using the software’s built-in procedure for non-parametric multiple comparisons, reporting two-tailed  $p$  values.

Survival distributions were estimated with the Kaplan–Meier method. Between-group differences in survival were evaluated using the log-rank test, implemented via the LifeLines package in Python [54]. The resulting  $p$  values from the log-rank test were adjusted for multiple comparisons using the Benjamini–Hochberg procedure to control the false discovery rate (FDR).

## 3 Results

Magnetic resonance imaging (MRI) of Long–Evans rats with intra-cerebrally implanted C6 gliomas revealed substantial heterogeneity in tumor development. Observed tumor volumes varied widely, ranging from minimal ( $< 2 \text{ mm}^3$ ) to extensive ( $> 320 \text{ mm}^3$ ).

### 3.1 Control nutritional regimen

The control nutritional regimen had no significant effect on either tumor growth rate (ANOVA:  $F(1, 24) = 0.001$ ,  $p = 0.969$ ) or survival (ANOVA:  $F(1, 28) = 0.455$ ,  $p = 0.505$ ).

### 3.2 Association between baseline anxiety-like behavior and tumor progression

Initial tumor growth rates, quantified via specific growth rate analysis from in vivo MRI performed on days 20–23 post-inoculation, were strongly associated with baseline anxiety-like behavior in the non-intervention group (ANOVA:  $F(2, 18) = 21.94$ ,  $p < 0.001$ ; Fig. 1c). Post hoc Bonferroni tests confirmed significant differences between high- and normal-anxiety subjects ( $p < 0.001$ ) and between normal- and low-anxiety subjects ( $p = 0.017$ ), while the high- and low-anxiety comparison was not significant ( $p = 0.132$ ). This finding was supported by non-parametric analysis (Kruskal–Wallis:  $H(2, N = 21) = 16.129$ ,  $p < 0.001$ , with a significant post hoc comparison between high and normal anxiety,  $p = 0.0002$ ).

This association was attenuated in the intervention group and did not reach statistical significance in the overall model (ANOVA:  $F(2, 12) = 3.34$ ,  $p = 0.07$ ; Kruskal–Wallis:  $H(2, N = 13) = 5.318$ ,  $p = 0.07$ ; Fig. 1d). However, a sex-stratified analysis within the intervention group revealed a significant main effect of anxiety level (ANOVA:  $F(2, 9) = 6.39$ ,  $p = 0.019$ ; Fig. 1e). Post hoc Bonferroni comparisons indicated significant differences between normal-anxiety females and both high-anxiety females ( $p = 0.018$ ) and low-anxiety males ( $p = 0.019$ ). The comparison between normal-anxiety females and high-anxiety males approached significance ( $p = 0.053$  with Bonferroni;  $p = 0.032$  with Tukey’s test). Non-parametric analysis within this stratified subset did not yield significant results.

### 3.3 Multivariate modeling of tumor progression and survival

A two-way ANOVA was conducted to assess the effects of baseline anxiety-like behavior (High, Normal, Low) and intervention timing (Pre-surgical, Post-surgical, Control) on tumor progression. Baseline anxiety had a significant

main effect on progression rate ( $F(2, 26) = 12.8, p < 0.001$ ). Dunnett's post hoc test, comparing all experimental groups to the non-intervention Control group, revealed significantly higher progression in the following groups relative to the Normal-anxiety Control: High-anxiety Control ( $p = 0.00003$ ), High-anxiety Pre-intervention ( $p = 0.008$ ), High-anxiety Post-intervention ( $p = 0.038$ ), and Low-anxiety Pre-intervention ( $p = 0.006$ ). Furthermore, progression in the Normal-anxiety Pre-intervention group was significantly lower than in the High-anxiety Control group ( $p = 0.002$ ).

This main effect of anxiety was corroborated by a non-parametric Kruskal–Wallis test across all subjects ( $H(2, N = 34) = 19.602, p < 0.001$ ), with a post hoc test confirming a significant difference between the aggregated High and Normal anxiety groups ( $p = 0.000029$ ; Fig. 2b).

In contrast, the association between baseline anxiety and survival was weaker and less consistent (ANOVA:  $F(2, 38) = 3.68, p = 0.035$ ; Kruskal–Wallis:  $H(2, N = 10) = 4.878, p = 0.087$ ; Fig. 2c).

Crucially, the behavioral intervention itself showed no significant main effect on either tumor progression ( $F(2, 26) = 0.55, p = 0.58$ ) or survival ( $F(2, 38) = 0.69, p = 0.51$ ). Furthermore, there was no significant interaction between baseline anxiety level and intervention timing for either progression ( $F(4, 26) = 1.52, p = 0.23$ ) or survival ( $F(4, 38) = 0.07, p = 0.99$ ).

### 3.4 Survival analysis using the Kaplan–Meier estimator

Kaplan–Meier analysis, with animals stratified by anxiety level, indicated significant differences in survival distributions (log-rank test:  $\chi^2 = 6.19, p = 0.045$ ; Fig. 2d). A subsequent pairwise comparison revealed a difference between the high- and normal-anxiety groups ( $\chi^2 = 4.89, p = 0.027$ ). This difference, however, did not remain statistically significant after correction for multiple comparisons using the Benjamini–Hochberg procedure (adjusted  $p = 0.08$ ). No other pairwise differences were significant.

### 3.5 Heterogeneity of tumor development

Longitudinal MRI documented instances of both absent tumor development ( $n = 4$ ) and spontaneous tumor regression ( $n = 3$ ) between 20 and 90 days post-inoculation (a representative case is illustrated in Fig. 2a). These cases were distributed across all behavioral groups (pre- or post-surgical learning and non-learning).

## 4 Discussion

### 4.1 Principal findings

Anxiety-like behavior was assessed using modified open field (mOFT) and novel object recognition (mNORT) tests. While the OFT is a widely used standardized paradigm, inter-laboratory variability can arise from differences in parameters such as arena geometry, illumination, and the criteria for identifying and interpreting behavioral events [55]. Consequently, behavioral phenotyping does not always yield directly comparable results across different experimental settings. In the present study, strict adherence to a detailed, standardized protocol enabled the acquisition of consistent and reproducible measurements across multiple experimenters. This internal consistency strengthens the validity of our core finding that individual differences in baseline behavior are critically linked to tumor growth dynamics. The results suggest that a reliably assessed behavioral phenotype can serve as a key stratifying variable, with its predictive value transcending specific methodological details as long as rigorous standardization is maintained within a given experimental framework.

The primary finding of this study is a significant, nonlinear relationship between baseline anxiety-like behavior and glioma progression, where extreme phenotypes were associated with the most aggressive tumor growth. This association was most pronounced in the absence of behavioral intervention, whereas an appetitive learning task attenuated this relationship by improving outcomes in a subset of high-anxiety subjects while worsening them in some with normal anxiety, thereby converging their trajectories. Importantly, the nutritional regimen linked to the intervention had no independent effect, confirming that the observed modulation was due to the behavioral and motivational context, rather than diet or the type of food.

These results support our central hypothesis derived from the theory of systemogenesis. Our data suggest that a high-anxiety phenotype may represent a state of chronic stress-induced cellular "reprogramming" conducive to tumor promotion. This provides a plausible explanation for the high variability in outcomes of exercise on tumor progression reported in the literature [46].

The observed link between anxiety and accelerated glioma growth aligns with established pathways of stress-mediated oncogenesis. Chronic stress, through glucocorticoid and catecholamine signaling, promotes an immunosuppressive TME, metabolic reprogramming, and disrupts genomic stability—processes particularly relevant in

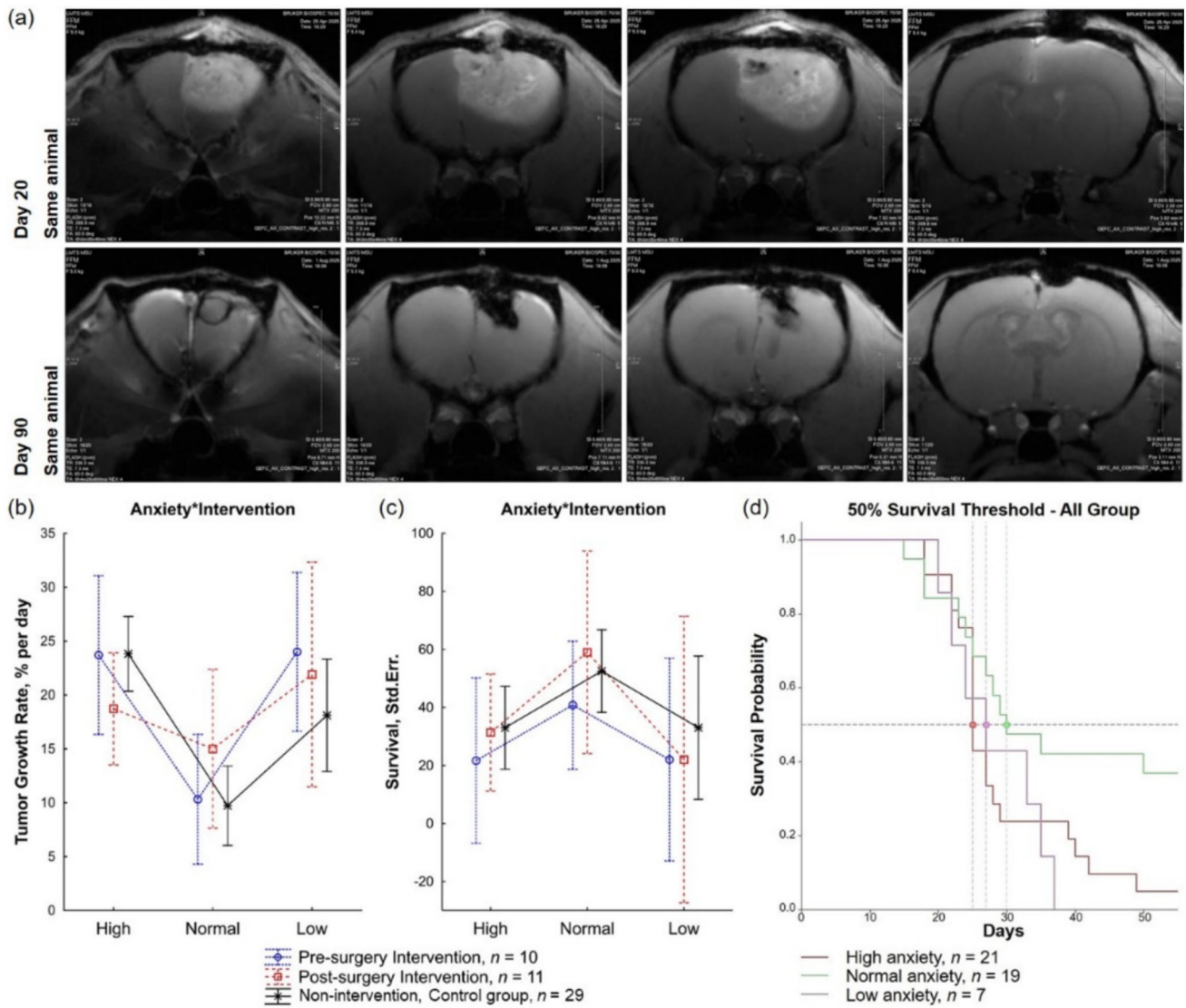


**Fig. 2** In vivo MRI monitoring of glioma progression and survival analysis. **a** Spontaneous tumor regression demonstrated by longitudinal axial T2-weighted MRI in a single rat at 20 and 90 days post-inoculation. **b, c** Relationship between anxiety-like behavior and tumor progression rate or survival, stratified by intervention status. Wide confidence intervals reflect high biological variability within the limited sample size. **b** Tumor growth rate, results of univariate analysis: Intercept ( $F = 311.3$ ,  $p < 0.001$ ), Anxiety ( $F = 12.8$ ,  $p < 0.001$ ), Intervention ( $F = 0.55$ ,  $p = 0.58$ ), Anxiety  $\times$  Intervention interaction ( $F = 1.52$ ,  $p = 0.23$ ). Dunnett's post hoc test: Normal Control versus High Pre-intervention,  $p = 0.008$ ; Normal Control versus High Post-intervention,  $p = 0.038$ ; Normal Control versus High Control,  $p = 0.00003$ ; Normal Control versus Low Pre-intervention,  $p = 0.006$ ; High Control versus Normal Pre-intervention,  $p = 0.002$ . Kruskal–Wallis:  $H(2, N = 34) = 19.602$ ,  $p < 0.001$ , High versus Normal,  $p = 0.000029$ . **c** Survival, results of univariate analysis: Intercept ( $F = 54.3$ ,  $p < 0.001$ ), Anxiety ( $F = 3.68$ ,  $p = 0.035$ ), Intervention ( $F = 0.69$ ,  $p = 0.51$ ), Anxiety  $\times$  Intervention interaction ( $F = 0.07$ ,  $p = 0.99$ ). Dunnett's test showed no significant pairwise differences for survival. Kruskal–Wallis:  $H(2, N = 10) = 4.878$ ,  $p = 0.087$ . **d** Kaplan–Meier survival curves stratified by anxiety level. The overall log-rank test indicated a significant difference between groups ( $\chi^2 = 6.19$ ,  $p = 0.045$ ). A subsequent pairwise comparison revealed a difference between the high- and normal-anxiety groups ( $\chi^2 = 4.89$ ,  $p = 0.027$ ), which did not remain significant after correction for multiple comparisons using the Benjamini–Hochberg procedure (adjusted  $p = 0.08$ )

glioma [18, 22, 26–32, 34, 35, 41]. Our findings extend this model by demonstrating that pre-existing, individual behavioral phenotypes can predict susceptibility to these pathways. The baseline anxiety level likely reflects an individual's neuro-immune and epigenetic "set point", influencing how the TME changes to both the challenge of a tumor and the context of a subsequent intervention.

The attenuation of the link between anxiety-like behavior and tumor progression by reward-contingent learning implies a specific modulation of the underlying neurobiological pathways. We posit that goal-directed, positively reinforced behavior may buffer the detrimental effects of chronic stress by engaging alternative signaling cascades and promoting adaptive epigenetic states. This conceptual framework aligns with established evidence demonstrating that distinct learning types can induce distinct brain-wide patterns of activity reorganization, as visualized through immediate-early gene mapping (e.g., *c-fos*) [3, 15, 44, 49].

The translational significance of this behavioral link is underscored by clinical evidence across cancer types. For instance, a systematic synthesis of evidence identifies structured physical activity as a key intervention associated with improved survival in breast cancer survivors, with proposed mechanisms including the modulation of chronic inflammation [56]. Clinical studies in glioblastoma patients reveal that higher pre-treatment scores on standardized scales for depression and anxiety correlate with poorer overall survival and a higher prevalence of tumor necrosis on MRI. Critically, ex vivo analysis demonstrated that primary glioblastoma cells from patients with these higher distress scores exhibited enhanced sphere-forming capacity, along with greater proliferative and invasive potential in functional assays, and distinct molecular profiles [57, 58]. This confluence of clinical and preclinical data reinforces the principle that an individual's psychological and behavioral phenotype is a critical determinant of disease progression. Consequently, clinical guidelines increasingly advocate for the integration of routine distress screening and psycho-oncological support, such as cognitive-behavioral therapy—which has demonstrated efficacy in ameliorating psychological symptoms in cancer patients—into standard care pathways [59].

Finally, MRI monitoring, conducted at 20 and 90 days post-inoculation, also revealed methodologically important cases that deviated markedly from the expected exponential growth pattern. In four rats, no tumor development was detected. In three other animals, we observed spontaneous tumor regression between days 20 and 90, culminating in the complete resolution of radiological signs. Critically, the uniform distribution of these outliers across all groups, including the non-intervention controls, implies that individual-specific factors—namely, the behavioral phenotype and its linked neuro-immune profile—play a decisive role in shaping the outcome through complex systemic interactions.

## 4.2 Limitations and future directions

Our study employed a two-week appetitive learning paradigm as a behavioral intervention. A key limitation of this design concerns the duration required for systemogenesis, a process encompassing learning and memory consolidation that includes, but is not limited to, adult neurogenesis, synaptogenesis, synaptic pruning, and apoptosis. The associated cellular signaling cascades documented in the literature can exert pronounced modulatory effects on the tumor microenvironment and, consequently, on tumor growth dynamics.

To isolate the specific effects of achievement-driven behavior with positive valence and motivation—serving as a model for cognitive-behavioral intervention—future studies should employ cohorts of pre-trained animals. This approach would allow a consolidated behavioral phenotype and its associated neural architecture to be established at least one month prior to tumor induction. This extended timeframe is necessary to accommodate well-characterized waves of gene expression following learning and new experiences, as well as the subsequent maturation and functional integration of new cellular adaptations into existing neuronal circuits.

Furthermore, future experimental designs must incorporate stringent controls for motor activity. A more complete understanding requires a bidirectional dissociation approach: comparing conditions matched for motivational goal but differing in locomotor intensity, as well as conditions with similar locomotor profiles but divergent motivational valences.

## 5 Conclusion and translational perspective

This study positions the individual behavioral phenotype as a potential stratifier for both cancer risk and response to behavioral therapy. The mitigation of chronic stress and the promotion of positively valenced experiences emerge as critical therapeutic targets. To test this hypothesis, future research must identify the precise neurobiological and immunological correlates linking varied motivational states to the dynamics of the oncological process.

Consequently, our findings argue for a paradigm shift toward personalized adjuvant strategies based on neuro-immunological profiling, motivated engagement, and controlled stress dynamics.

**Acknowledgements** MRI studies were conducted under the state assignment of Lomonosov Moscow State University.

## Author contributions

Conceptualization and methodology: Yuri I. Alexandrov and Alexandra I. Bulava; Formal analysis and investigation: Alexandra I. Bulava, Vera V. Kudelkina, Mikhail V. Gulyaev, Vladimir D. Ilyushichev, Natalia A. Chistova, Zhanna A. Osipova, Vladimir B. Dorokhov; Writing—original draft preparation: Alexandra I. Bulava; Writing—editing: Vera V. Kudelkina and Yuri I. Alexandrov; Supervision: Yuri I. Alexandrov.

**Funding** The research leading to these results received funding from the Russian Science Foundation (project No. 23–18–00801), Institute of Psychology RAS.

**Data availability** All data generated and analyzed during this study are maintained in the laboratory’s database. They are available from the corresponding author upon reasonable request.

## Declarations

**Conflict of interest** The authors have no competing interests to declare that are relevant to the content of this article.

## References

1. Y.I. Alexandrov, M.V. Pletnikov, Neuronal metabolism in learning and memory: the anticipatory activity perspective. *Neurosci. Biobehav. Rev.* **137**, 104664 (2022). <https://doi.org/10.1016/j.neubiorev.2022.104664>
2. Y.I. Alexandrov, A.A. Sozinov, O.E. Svarnik, A.G. Gorkin, E.A. Kuzina, V.V. Gavrilov, K.R. Arutyunova, Determination of neuronal activity and its meaning for the processes of learning and memory, in *Systems Neuroscience. Adv. Neurobiol.*, vol. 41 ed. by A.CH. Yu, K. Gao, J. Zhan (Springer, Cham, 2024). [https://doi.org/10.1007/978-3-031-69188-1\\_1](https://doi.org/10.1007/978-3-031-69188-1_1)
3. A.I. Bulava, Y.I. Alexandrov, Relationship between the BDNF level in areas of the medial prefrontal cortex of rats during motivation-driven learning of a formed behavior: approach/avoidance. *Neurosci. Behav. Physiol.* **55**, 961–967 (2025). <https://doi.org/10.1007/s11055-025-01851-7>
4. A.A. Venerin, Y.A. Venerina, Y.I. Alexandrov, Cell functioning in norm and pathology in terms of the activity paradigm: oncogenesis. *Med. Hypotheses* **144**, 110240 (2020). <https://doi.org/10.1016/j.mehy.2020.110240>
5. Y.I. Alexandrov, A.I. Bulava, A.V. Bakhchina, V.V. Gavrilov, M.G. Kolbeneva, E.A. Kuzina, I.I. Znamenskaya, I.I. Rusak, A.G. Gorkin, Stress and individual development. *Neurosci. Behav. Physiol.* **53**(1), 47–60 (2023). <https://doi.org/10.1007/s11055-023-01390-z>
6. J. Park, B. Moghaddam, Impact of anxiety on prefrontal cortex encoding of cognitive flexibility. *Neurosci. Cognit. Flexibil. Dev. Dis. Treat.* **345**, 193–202 (2017). <https://doi.org/10.1016/j.neuroscience.2016.06.013>
7. A.I. Bulava, Z.A. Osipova, V.V. Arapov, A.G. Gorkin, I.O. Alexandrov, T.N. Grechenko, Y.I. Alexandrov, The influence of anxiety and exploratory activity on learning in rats: mismatch-induced c-fos expression in deep and superficial cortical layers, in *Advances in Neural Computation, Machine Learning, and Cognitive Research VII. Stud. Comput. Intell.*, vol. 1120 (Springer, Cham, 2023), pp. 323–333. [https://doi.org/10.1007/978-3-031-44865-2\\_35](https://doi.org/10.1007/978-3-031-44865-2_35)
8. Y. Alexandrov, B. Feldman, O. Svarnik, I. Znamenskaya, M. Kolbeneva, K. Arutyunova, A. Krylov, A. Bulava, Regression I. Experimental approaches to regression. *J. Anal. Psychol.* **65**(2), 345–365 (2020). <https://doi.org/10.1111/1468-5922.12580>
9. Y. Alexandrov, B. Feldman, O. Svarnik, I. Znamenskaya, M. Kolbeneva, K. Arutyunova, A. Krylov, A. Bulava, Regression II. Development through regression. *J. Anal. Psychol.* **65**(3), 476–496 (2020). <https://doi.org/10.1111/1468-5922.12596>
10. B. Nadarajah, J.G. Parnavelas, Modes of neuronal migration in the developing cerebral cortex. *Nat. Rev. Neurosci.* **3**, 423–432 (2002). <https://doi.org/10.1038/nrn845>
11. S. Siso et al., Editor’s highlight: spatiotemporal progression and remission of lesions in the rat brain following acute intoxication with diisopropylfluorophosphate. *Toxicol. Sci.* **157**(2), 330–341 (2017). <https://doi.org/10.1093/toxsci/kf x048>
12. L. Schwabe, O.T. Wolf, Stress and multiple memory systems: from ‘thinking’ to ‘doing.’ *Trends Cogn. Sci.* **17**(2), 60–68 (2013). <https://doi.org/10.1016/j.tics.2012.12.001>
13. T. Lissek, Activity-dependent induction of younger biological phenotypes. *Adv. Biol.* **6**, 2200119 (2022). <https://doi.org/10.1002/adbi.202200119>
14. C.H. Lineweaver, K.J. Bussey, A.C. Blackburn, P.C. Davies, Cancer progression as a sequence of atavistic reversions. *BioEssays* **43**(7), 2000305 (2021). <https://doi.org/10.1002/bies.202000305>
15. A. Bulava, Y. Alexandrov, Reconsolidation and cognitive novelty, in: *Advances in Cognitive Research, Artificial Intelligence and Neuroinformatics. Adv. Intell. Syst. Comput.*, vol. 1358. (Springer, Cham, 2021), pp. 504–509. <https://doi.org/10.1007/978-3-030-71637-0>
16. A. Shomar, O. Barak, N. Brenner, Cancer progression as a learning process. *iScience* **25**(3), 103924 (2022). <https://doi.org/10.1016/j.isci.2022.103924>

17. N.V. Gulyaeva, Glucocorticoids orchestrate adult hippocampal plasticity: growth points and translational aspects. *Biochem. Mosc.* **88**, 565–589 (2023). <https://doi.org/10.1134/S0006297923050012>
18. C.S. Leung, O. Kosyk, E.M. Welter, N. Dietrich, T.K. Archer, A.S. Zannas, Chronic stress-driven glucocorticoid receptor activation programs key cell phenotypes and functional epigenomic patterns in human fibroblasts. *iScience* **25**(9), 104960 (2022). <https://doi.org/10.1016/j.isci.2022.104960>
19. S. Bhattacharya, H. Makkar, J.P. Meena, A.K. Gupta, R. Seth, Epigenetic paradigm of DNA methylation for understanding the pathophysiology, diagnostics, and therapeutics in sarcomas. *Epigenomics* **17**(16), 1213–1224 (2025). <https://doi.org/10.1080/17501911.2025.2563500>
20. M. Colón-Cesario, J. Wang, X. Ramos, H.G. García, J.J. Dávila, J. Laguna, C. Rosado, S. de Peña Ortiz, S.P. de Ortiz, An inhibitor of DNA recombination blocks memory consolidation, but not reconsolidation, in context fear conditioning. *J. Neurosci.* **26**(20), 5524–5533 (2006). <https://doi.org/10.1523/JNEUROSCI.3050-05.2006>
21. F. Winkler, H.S. Venkatesh, M. Amit, T. Batchelor, I.E. Demir, B. Deneen, M. Monje et al., Cancer neuroscience: state of the field, emerging directions. *Cell* **186**(8), 1689–1707 (2023). <https://doi.org/10.1016/j.cell.2023.02.002>
22. A. Seiler, A.K. Sood, J. Jenewein, C.P. Fagundes, Can stress promote the pathophysiology of brain metastases? A critical review of biobehavioral mechanisms. *Brain Behav. Immun.* **87**, 860–880 (2020). <https://doi.org/10.1016/j.bbi.2019.12.013>
23. P. Radley, Preclinical models of chronic stress: adaptation or pathology? *Biol. Psychiatry* **94**, 194–202 (2023). <https://doi.org/10.1016/j.biopsych.2022.11.004>
24. F. Li, M.C. Simon, Cancer cells don't live alone: metabolic communication within tumor microenvironments. *Dev. Cell* **54**(2), 183–195 (2020). <https://doi.org/10.1016/j.devcel.2020.06.018>
25. G. Qiao, M. Chen, H. Mohammadpour, C.R. MacDonald, M.J. Bucsek et al., Chronic adrenergic stress contributes to metabolic dysfunction and an exhausted phenotype in T cells in the tumor microenvironment. *Cancer Immunol. Res.* **9**(6), 651–664 (2021). <https://doi.org/10.1158/2326-6066.CIR-20-0445>
26. H. Yang, L. Xia, J. Chen, S. Zhang, V. Martin, Q. Li, Y. Ma et al., Stress–glucocorticoid–TSC2D3 axis compromises therapy-induced antitumor immunity. *Nat. Med.* **25**(9), 1428–1441 (2019). <https://doi.org/10.1038/s41591-019-0566-4>
27. J. Chen, J. Li, H. Qiao, R. Hu, C. Li, Disruption of IDO signaling pathway alleviates chronic unpredictable mild stress-induced depression-like behaviors and tumor progression in mice with breast cancer. *Cytokine* **162**, 156115 (2023). <https://doi.org/10.1016/j.cyto.2022.156115>
28. B.W. Renz, R. Takahashi, T. Tanaka, M. Macchini, Y. Hayakawa, Z. Dantes, T.C. Wang et al.,  $\beta$ 2 adrenergic-neurotrophin feedforward loop promotes pancreatic cancer. *Cancer Cell* **33**(1), 75–90 (2018). <https://doi.org/10.1016/j.ccell.2017.11.007>
29. A. Eckerling, I. Ricon-Becker, L. Sorski, E. Sandbank, S. Ben-Eliyahu, Stress and cancer: mechanisms, significance and future directions. *Nat. Rev. Cancer* **21**(12), 767–785 (2021). <https://doi.org/10.1038/s41568-021-00395-5>
30. J.K. Allen, G.N. Armaiz-Pena, A.S. Nagaraja, N.C. Sadaoui, T. Ortiz, R. Dood, M. Ozcan, D.M. Herder, M. Haemmerle, K.M. Gharpure, R. Rupaimoole, R.A. Previs, S.Y. Wu, S. Pradeep, X. Xu, H.D. Han, B. Zand, H.J. Dalton, M. Taylor, W. Hu, J. Bottsford-Miller, M. Moreno-Smith, Y. Kang, L.S. Mangala, C. Rodriguez-Aguayo, V. Sehgal, E.L. Spaeth, P.T. Ram, S.T.C. Wong, F.C. Marini, G. Lopez-Berestein, S.W. Cole, S.K. Lutgendorf, M. De Biasi, A.K. Sood, Sustained adrenergic signaling promotes intratumoral innervation through BDNF induction. *Cancer Res.* **78**(12), 3233–3242 (2018). <https://doi.org/10.1158/0008-5472.CAN-16-1701>
31. A.H. Marques, M.N. Silverman, E.M. Sternberg, Glucocorticoid dysregulations and their clinical correlates: from receptors to therapeutics. *Ann. N. Y. Acad. Sci.* **1179**(1), 1–18 (2009). <https://doi.org/10.1111/j.1749-6632.2009.04987.x>
32. M.M.S. Obradović, B. Hamelin, N. Manevski et al., Glucocorticoids promote breast cancer metastasis. *Nature* **567**, 540–544 (2019). <https://doi.org/10.1038/s41586-019-1019-4>
33. M. Napoli, J.E. Girardini, S. Piazza et al., Wiring the oncogenic circuitry: Pin1 unleashes mutant p53. *Oncotarget* **2**(9), 654–656 (2011). <https://doi.org/10.18632/oncotarget.329>
34. Y. Zhao, Y. Jia, T. Shi, W. Wang, D. Shao, X. Zheng et al., Depression promotes hepatocellular carcinoma progression through a glucocorticoid-mediated upregulation of PD-1 expression in tumor-infiltrating NK cells. *Carcinogenesis* **40**(9), 1132–1141 (2019). <https://doi.org/10.1093/carcin/bgz017>
35. R. Muthuswamy, N.J. Okada, F.J. Jenkins, K. McGuire, P.F. McAuliffe, H.J. Zeh, D.L. Bartlett et al., Epinephrine promotes COX-2-dependent immune suppression in myeloid cells and cancer tissues. *Brain Behav. Immun.* **62**, 78–86 (2017). <https://doi.org/10.1016/j.bbi.2017.02.008>
36. J. Du, H. Qin, Lipid metabolism dynamics in cancer stem cells: potential targets for cancers. *Front. Pharmacol.* **15**, 1367981 (2024). <https://doi.org/10.3389/fphar.2024.1367981>
37. S.A. Polyzos, G. Targher, Role of glucocorticoids in metabolic dysfunction-associated steatotic liver disease. *Curr. Obes. Rep.* **13**, 242–255 (2024). <https://doi.org/10.1007/s13679-024-00556-1>
38. M. Vicario, M. Guilarte, C. Alonso, P. Yang, C. Martínez, L. Ramos, B. Lobo et al., Chronological assessment of mast cell-mediated gut dysfunction and mucosal inflammation in a rat model of chronic psychosocial stress. *Brain Behav. Immun.* **24**(7), 1166–1175 (2010). <https://doi.org/10.1016/j.bbi.2010.06.002>
39. L. Zhao, X. Hou, Y. Feng, Y. Zhang, S. Shao, X. Wu, J.J. Zhang, Z. Zhang, A chronic stress-induced microbiome perturbation, highly enriched in Ruminococcaceae\_UCG-014, promotes colorectal cancer growth and metastasis. *Int. J. Med. Sci.* **21**(5), 882–895 (2024). <https://doi.org/10.7150/ijms.90612>

40. Q. Wang, J. Liu, M. Yang, J. Zhou, Y. Li, J. Zheng et al., Targeting AKR1B1 inhibits metabolic reprogramming to reverse systemic therapy resistance in hepatocellular carcinoma. *Signal Transduct. Target. Ther.* **10**(1), 244 (2025). <https://doi.org/10.1038/s41392-025-02321-9>
41. B. Huang, H. An, H. Wu, Y. Qiu, Y. Su, L. Chen et al., Chronic psychological stress in oncogenesis: multisystem crosstalk and multimodal interventions. *Research* **8**, 0948 (2025). <https://doi.org/10.34133/research.0948>
42. C. Westlin, J.E. Theriault, Y. Katsumi, A. Nieto-Castanon, A. Kucyi, S.F. Ruf, S.M. Brown, M. Pavel, D. Erdogmus, D.H. Brooks, K.S. Quigley, S. Whitfield-Gabrieli, L.F. Barrett, Improving the study of brain-behavior relationships by revisiting basic assumptions. *Trends Cogn. Sci.* **27**(3), 246–257 (2023)
43. K.G. Cruz, Y.N. Leow, N.M. Le, E. Adam, R. Huda, M. Sur, Cortical-subcortical interactions in goal-directed behavior. *Physiol. Rev.* **103**(1), 347–389 (2023). <https://doi.org/10.1152/physrev.00048.2021>
44. S.Y. Lara Aparicio, Ád.J. Laureani Fierro, G.E. Aranda Abreu, R. Toledo Cárdenas, L.I. García Hernández, G.A. Coria Ávila, F. Rojas Durán, M.E.H. Aguilar, J. Manzo Denes, L.D. Chi-Castañeda, C.A. Pérez Estudillo, Current opinion on the use of c-Fos in neuroscience. *NeuroSci* **3**(4), 687–702 (2022). <https://doi.org/10.3390/neurosci3040050>
45. A. Papadopetraki, M. Maridaki, F. Zagouri, M.A. Dimopoulos, M. Koutsilieris, A. Philippou, Physical exercise restrains cancer progression through muscle-derived factors. *Cancers* **14**(8), 1892 (2022). <https://doi.org/10.3390/cancers14081892>
46. R.C.K.R. Eschke, A. Lampit, A. Schenk, F. Javelle, K. Steindorf, P. Diel, P. Zimmer et al., Impact of physical exercise on growth and progression of cancer in rodents—a systematic review and meta-analysis. *Front. Oncol.* **9**, 35 (2019). <https://doi.org/10.3389/fonc.2019.00035>
47. V.V. Kudelkina, A.M. Kosyreva, O.S. Pavlova, M.V. Gulyaev, A.E. Umryukhin, Z.A. Nefedova, A.I. Bulava, A.G. Gorkin, Models of high-grade glioma in rats: morphology, size, thickness of cerebral cortex, and survival. *Bull. Exp. Biol. Med.* **179**, 490–495 (2025). <https://doi.org/10.1007/s10517-025-06516-6>
48. V. Kudelkina, A. Bulava, A. Gorkin, Y. Venerina, Y. Alexandrov, Comparative characterization of high-grade glioma models in rats: importance for neurobiology. *Clin. Transl. Neurosci.* **9**(4), 58 (2025). <https://doi.org/10.3390/ctn9040058>
49. O.E. Svarnik, A.I. Bulava, Y.I. Alexandrov, Expression of c-Fos in the rat retrosplenial cortex during instrumental re-learning of appetitive bar-pressing depends on the number of stages of previous training. *Front. Behav. Neurosci.* **7**, 78 (2013). <https://doi.org/10.3389/fnbeh.2013.00078>
50. A.I. Bulava, S.V. Volkov, Y.I. Alexandrov, A novel avoidance test setup: device and exemplary tasks. in *Advances in Neural Computation, Machine Learning, and Cognitive Research III. Stud. Comput. Intell.*, vol. 856, ed. by B. Kryzhanovskiy, W. Dunin-Barkowski, V. Redko, Y. Tiumentsev (Springer, Cham, 2020) , pp. 159–164. [https://doi.org/10.1007/978-3-030-30425-6\\_18](https://doi.org/10.1007/978-3-030-30425-6_18)
51. R. Landgraf, A. Wigger, High vs low anxiety-related behavior rats: an animal model of extremes in trait anxiety. *Behav. Genet.* **32**, 301–314 (2002). <https://doi.org/10.1023/A:1020258104318>
52. M. Antunes, G. Biala, The novel object recognition memory: neurobiology, test procedure, and its modifications. *Cogn. Process.* **13**, 93–110 (2012). <https://doi.org/10.1007/s10339-011-0430-z>
53. E. Mehrara, E. Forssell-Aronsson, H. Ahlman, P. Bernhardt, Specific growth rate versus doubling time for quantitative characterization of tumor growth rate. *Cancer Res.* **67**(8), 3970–3975 (2007). <https://doi.org/10.1158/0008-5472.CAN-06-3822>
54. C. Davidson-Pilon, Lifelines: survival analysis in Python. *J. Open Source Softw.* **4**(40), 1317 (2019). <https://doi.org/10.21105/joss.01317>
55. L. Lewejohann, C. Reinhard, A. Schrewe, J. Brandewiede, A. Haemisch, N. Görtz, N. Sachser et al., Environmental bias? Effects of housing conditions, laboratory environment and experimenter on behavioral tests. *Genes Brain Behav.* **5**(1), 64–72 (2006). <https://doi.org/10.1111/j.1601-183X.2005.00140.x>
56. L. Yeganeh, S. Willey, C.S. Wan et al., The effects of lifestyle and behavioural interventions on cancer recurrence, overall survival and quality of life in breast cancer survivors: a systematic review and network meta-analysis. *Maturitas* **185**, 107977 (2024). <https://doi.org/10.1016/j.maturitas.2024.107977>
57. A. Ley, M. Kamp, C. von Sass et al., Psychooncological distress in low-grade glioma patients—a monocentric study. *Acta Neurochir.* **164**, 713–722 (2022). <https://doi.org/10.1007/s00701-021-04863-7>
58. X. Fu, C. Wu, N. Han et al., Depressive and anxiety disorders worsen the prognosis of glioblastoma. *Aging (Albany NY)* **12**(20), 20095–20110 (2020). <https://doi.org/10.18632/aging.103593>
59. L. Zhang, X. Liu, F. Tong et al., Cognitive behavioral therapy for anxiety and depression in cancer survivors: a meta-analysis. *Sci. Rep.* **12**, 21466 (2022). <https://doi.org/10.1038/s41598-022-25068-7>

Springer Nature or its licensor (e.g. a society or other partner) holds exclusive rights to this article under a publishing agreement with the author(s) or other rightsholder(s); author self-archiving of the accepted manuscript version of this article is solely governed by the terms of such publishing agreement and applicable law.